



Originally published as:

Maystrenko, Y., Scheck-Wenderoth, M. (2009): Density contrasts in the upper mantle and lower crust across the continent–ocean transition: constraints from 3-D gravity modelling at the Norwegian margin. - *Geophysical Journal International*, 179, 1, pp. 536—548.

DOI: <http://doi.org/10.1111/j.1365-246X.2009.04273.x>

Density contrasts in the upper mantle and lower crust across the continent–ocean transition: constraints from 3-D gravity modelling at the Norwegian margin

Yuriy Maystrenko and Magdalena Scheck-Wenderoth

Deutsches GeoForschungsZentrum Potsdam GFZ, Telegrafenberg, 14473 Potsdam, Germany. E-mail: yuram@gfz-potsdam.de

Accepted 2009 May 27. Received 2009 May 14; in original form 2008 April 30

SUMMARY

3-D gravity models that consider the highly complex density structure of the Norwegian passive volcanic continental margin require a significantly lower density in the mantle below the ocean than below the continent. This is especially pronounced on the crust-free residual gravity anomalies obtained by 3-D gravity stripping. This density contrast in the mantle indicates different physical properties either related to thermal or compositional conditions beneath the two domains. We assess the gravity response of thermal differences and find that a hotter oceanic mantle compared to a colder continental mantle could cause the density contrast. Accordingly, 3-D lithospheric-scale gravity models considering temperature-dependent mantle densities indicate that the transition between continental and oceanic lithosphere is rather sharp with a steep gradient in thickness beneath the continent–ocean transition zone. Furthermore, a mantle wedge of reduced density extends from the oceanic Jan Mayen Fracture Zone to the continental Jan Mayen Lineament and points to increased mantle temperatures and/or compositional changes beneath the lineament. The models further indicate the presence of high-density bodies within the lower crust at the continent–ocean transition that are continuous with the lowermost oceanic layer 3B in terms of geometry and density. This supports the concept of underplated lower crust beneath the western Norwegian margin. Finally, NE–SW trending linear zones of increased density are required in the lower crust beneath the eastern Vøring and Møre Basins to fit the short-wavelength gravity signal.

Key words: Gravity anomalies and Earth structure; Continental margins: divergent; Sedimentary basin processes; Dynamics of lithosphere and mantle; Crustal structure; Atlantic Ocean.

1 INTRODUCTION

The detailed structure of the deeper crust and mantle below passive continental margins and especially at the continent–ocean transition is still a matter of debate. As the Norwegian continental margin is very well explored this topic can be studied there in great detail, and in particular in 3-D (Fig. 1). The margin formed between the exposed Fennoscandian Caledonides in the east and the Cenozoic oceanic domain of the North Atlantic in the west as a result of several rifting events after post-Caledonian collapse (Blystad *et al.* 1995). By far the largest part of the up to 18-km-thick sedimentary succession was deposited before continental breakup in the Late Palaeocene–Early Eocene (~55 Ma). Structurally, the Norwegian continental margin is segmented into the Trøndelag Platform, adjacent to the Norwegian coast and containing thick Pre-Cretaceous sediments, followed westward by the Cretaceous Vøring and Møre Basins, which are separated from the oceanic crust by the Vøring and Møre Marginal Highs (Blystad *et al.* 1995). Though different models have

been proposed to explain the observed gravity signal of the margin (Torne *et al.* 2003; Fernandez *et al.* 2005; Mjelde *et al.* 2005; Ebbing *et al.* 2006; Raum *et al.* 2006), previous models did not consider the influence of the oceanic part of the system in 3-D.

The sedimentary infill of the Norwegian margin is particularly well known due to oil and gas prospecting and scientific studies (Blystad *et al.* 1995; Brekke 2000; Ren *et al.* 2003), but the deep crustal structure has also been intensively explored by deep seismic sounding (Mjelde *et al.* 1997, 2001, 2005, 2009; Raum *et al.* 2002; Raum *et al.* 2006). A recently developed, crustal-scale 3-D structural model of the Norwegian margin (Scheck-Wenderoth *et al.* 2007) integrates many of these results (Fig. 2). Though the upper part of this model is well constrained, uncertainties exist in the lower crust and mantle, related to the decreasing data density with depth. We use this 3-D structural model as a starting point for our study and apply combined gravity and thermal modelling to further evaluate the configuration of the lower crust and the lithospheric mantle beneath the margin and the continent–ocean transition.

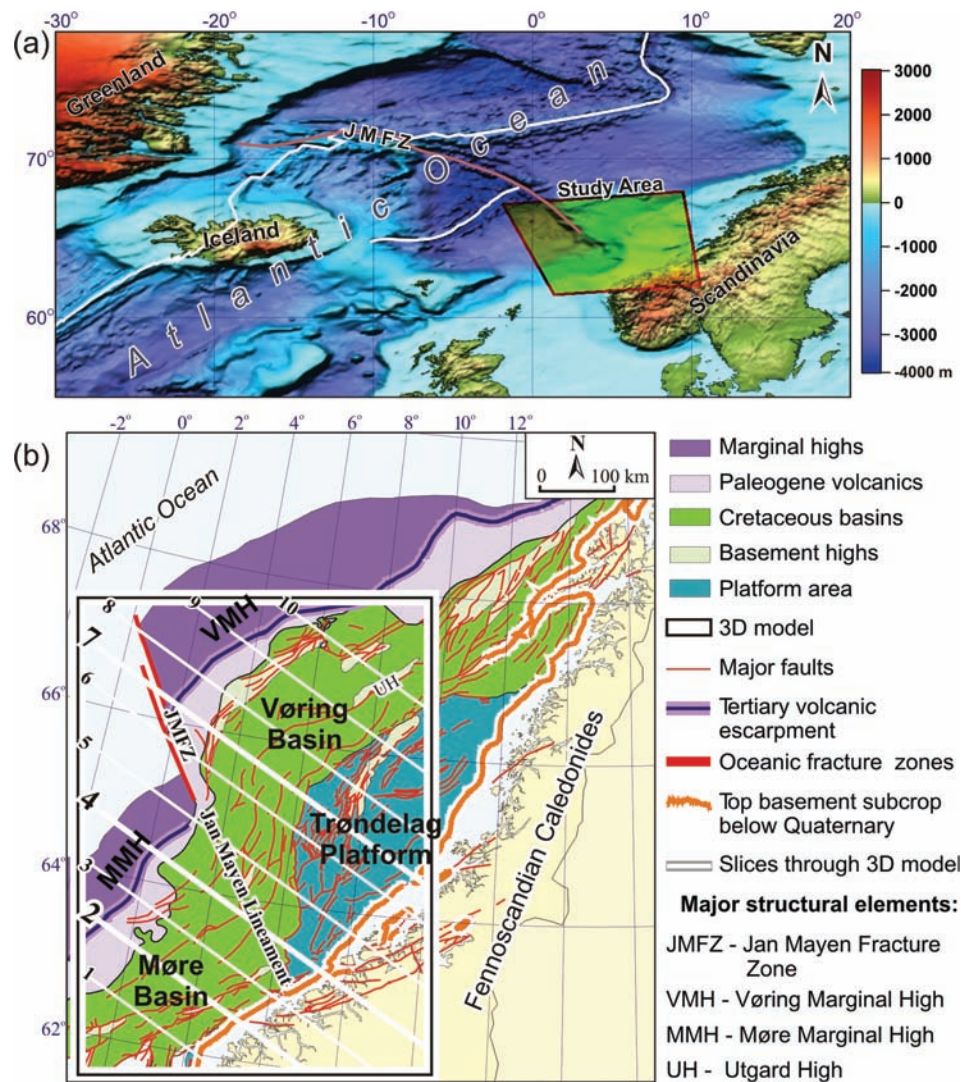


Figure 1. (a) Location of the study area within the Northern Atlantic (the bathymetry is reproduced from the GEBCO Digital Atlas published by the British Oceanographic Data Centre on behalf of IOC and IHO; IOC, IHO and BODC 2003; position of plate boundaries and Jan Mayen Fracture Zone after Müller *et al.* 1997); (b) Structural map of the Norwegian continental shelf (simplified after Blystad *et al.* 1995) with location of the vertical slices through 3-D model.

2 DATA AND METHOD

2.1 The 3-D structural model

The 3-D structural model (Scheck-Wenderoth *et al.* 2007) we use as a starting point for this study is based on the data shown in Fig. 2. For the sedimentary infill five maps of the major Cretaceous–Cenozoic unconformities in two-way traveltimes (TWT) and related fault maps (Brekke 2000) were available. The TWT thicknesses of the layers between these unconformities were calculated as the difference between the structural time maps. The obtained TWT thickness maps have been gridded with a cell resolution of $2.5 \text{ km} \times 2.5 \text{ km}$ and depth-converted by use of interval velocities (Scheck-Wenderoth *et al.* 2007). In addition, deep well data (NPD 2007) were used to crosscheck the thicknesses of the sedimentary layers.

For the crystalline crust, the initial dataset consists of six depth levels of crustal layers from long-offset seismic refraction profiles (magenta lines in Fig. 2) recorded with ocean bottom seismometers (OBS; Mjelde *et al.* 1997, 2001, 2002, 2003, 2005; Raum 2000; Raum *et al.* 2002, 2006). The base (crust–mantle boundary–Moho)

and top of the crystalline crust (base of sediments) have been extracted from this dataset. Likewise, the thickness of a high-velocity body in the lower continental crust below the western Vøring Basin and the thicknesses of three oceanic crustal layers were obtained from the OBS data. Finally, data from inversion of teleseismic receiver functions (Ottemöller & Midzi 2003; blue squares in Fig. 2) have been used to control the depth of the Moho below the continent where no deep refraction data were available.

All datasets were gridded and integrated into a 3-D structural model. In some areas, where data coverage is poor, interpolation has been used to fill data gaps. Thus, the input 3-D model includes thirteen layers: sea water; a post- and a pre-Mid-Miocene layer, a layer of Palaeocene; oceanic layers 2AB, 3A and 3B, two layers of Cretaceous, a pre-Cretaceous sedimentary layer, a layer of continental crystalline crust, a continental lower crustal high-velocity body below only the western Vøring Basin and an upper mantle layer.

The sedimentary fill of the margin is built up of three structural levels. The uppermost level of Cenozoic, mainly post-breakup deposits found over the entire margin attains more than 3 km of thickness in two major depocentres (Fig. 3a). Under the Base

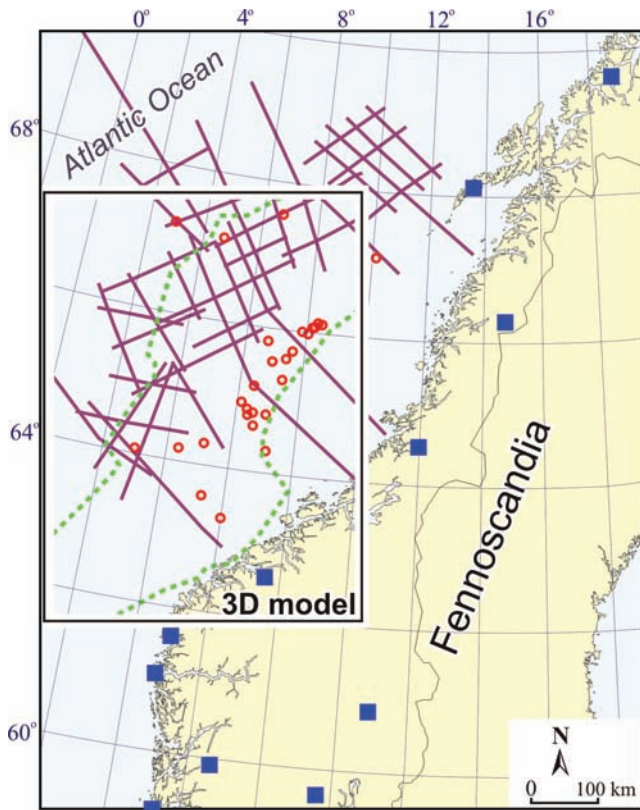


Figure 2. Data used for the construction of the 3-D structural model of the Norwegian continental margin (Scheck-Wenderoth *et al.* 2007). Red circles are deep wells (NPD 2007); green dotted lines outline the area which is covered by published maps of sedimentary interfaces (Brekke 2000); magenta lines are OBS data (Mjelde *et al.* 1997, 2001, 2002, 2003, 2005; Raum *et al.* 2000, 2002, 2006); and blue squares are published results from inversion of teleseismic receiver functions (Ottemöller & Midzi 2003).

Cenozoic Unconformity, up to 12 km of Cretaceous sediments are present in the Vøring and Møre Basins, which together form a NNE-SSW oriented basin (Fig. 3b). Below, up to 12 km of pre-Cretaceous deposits include mainly Permian–Jurassic sediments (Fig. 3c) on the Trøndelag Platform and beneath the western Vøring and Møre Basins.

Table 1. Velocity and density values of the sedimentary, crustal and mantle layers of 3-D model.

Layer	Velocity (m s ⁻¹)	Density (kg m ⁻³)
Tertiary	1800–2300	1950–2250
Cretaceous	3000–5300	2430–2600
Pre-Cretaceous	5000–5500	2650
Continental crystalline crust	6000–6700	2780
Continental crystalline crust	6000–6700	2780
Continental crystalline crust	6000–6700	2780
Continental high-velocity (density) body	7100–7600	3150
Continental high-density zones	Undefined	3110
Continental mantle	8000–8300	3330
Oceanic layer 2AB	4000–6000	2650
Oceanic layer 3A	6000–6700	2890
Oceanic layer 3B	7100–7600	3150
Oceanic mantle	7800–8000	3180

The top of the crystalline basement crops out onshore in Norway and successively steps down to the west, lying about 8 km deep below the Trøndelag Platform and 18 km deep below the western Vøring and Møre Basins, the latter showing local basement highs along the basin axes (Ebbing *et al.* 2006; Scheck-Wenderoth *et al.* 2007). Furthermore, the high-velocity body found from deep refraction seismic data was included below the western Vøring Basin (Mjelde *et al.* 2001, 2005; Raum *et al.* 2006).

The oceanic crust below the Cenozoic sediments has a three-layered structure with all oceanic layers thickened beneath the Vøring and Møre Marginal Highs. Following the interpretation of Mjelde *et al.* (2005) and Raum *et al.* (2006), the upper layer 2AB is interpreted to consist mainly of flood basalts and diabase dikes, the middle layer 3A is assumed to be a mixture of sheeted dykes and gabbroic intrusions and the lowest oceanic layer 3B has the properties of gabbros and ultramafic rocks. This lowermost oceanic layer 3B appears to be continuous with the high-velocity body observed in the lower crust beneath the Vøring Basin in terms of seismic velocities, thickness and depth position (Table 1; Mjelde *et al.* 1997, 2005; Raum *et al.* 2002, 2006; Scheck-Wenderoth *et al.* 2007).

An apparent left-lateral offset is observed between the marginal highs and the thickness maxima of the oceanic and lower crustal layers along the Jan Mayen Fracture Zone and its continental continuation, the Jan Mayen Lineament (Fig. 1a), which is a

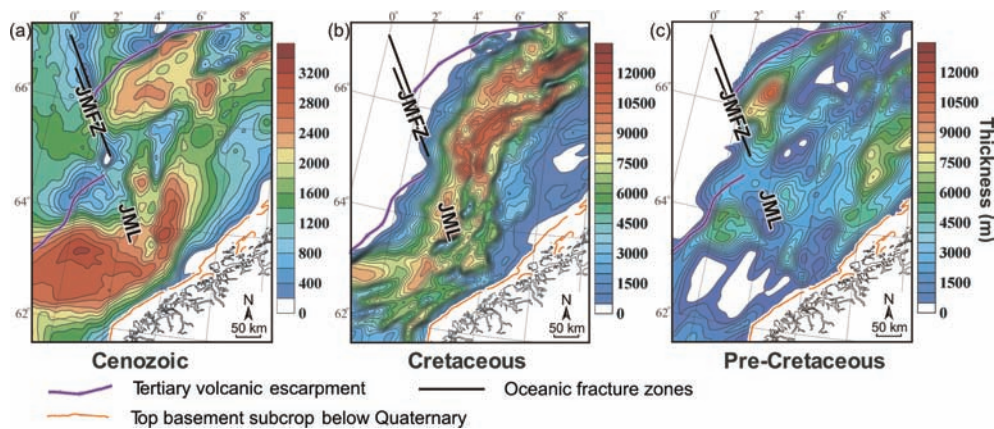


Figure 3. Present-day thickness maps of sediment packages: (a) Cenozoic, (b) Cretaceous and (c) Pre-Cretaceous (after Scheck-Wenderoth *et al.* 2007). JMFZ: Jan Mayen Fracture Zone, JML: Jan Mayen Lineament.

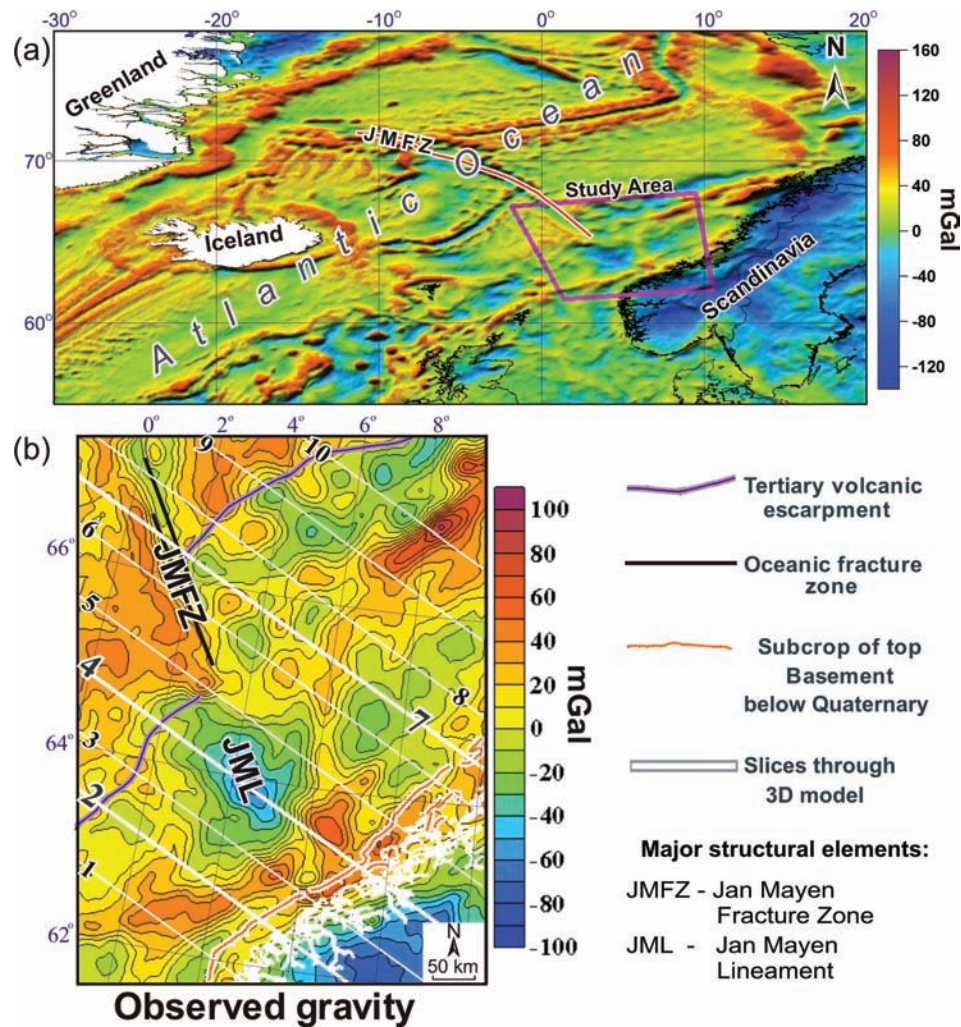


Figure 4. (a) Gravity anomaly over the North Atlantic area (Sandwell & Smith 1997; Wybraniec *et al.* 1998). (b) Gravity anomaly over the Norwegian continental margin and adjacent areas with location of the vertical slices through 3-D structural model (Wybraniec *et al.* 1998). In both maps: Bouguer gravity anomalies onshore and Free-Air anomalies offshore. JMFZ: Jan Mayen Fracture Zone, JML: Jan Mayen Lineament.

prominent structure in the sedimentary section as well (Fig. 3). Berndt *et al.* (2001) have shown that the Jan-Mayen Fracture Zone is a deep-seated discontinuity and separates the syn-breakup volcanic complexes which cover the Vøring and Møre Marginal Highs. Furthermore, Torske & Prestvik (1991) put forward the hypothesis that the continental Jan Mayen Lineament may have played a major role during the pre-break up extensional history of the Vøring and Møre Basins.

2.2 Gravity field

The free-air anomaly offshore and the Bouguer gravity anomaly onshore (Fig. 4; Sandwell & Smith 1997; Wybraniec *et al.* 1998) show pronounced gravity lows over Scandinavia and over the continental shelf of Greenland (Fig. 4a). On the other hand, the gravity field over the North Atlantic Ocean is characterized by an increased gravity compared to the continental parts. There is a clear correlation between the topography of the sea floor and some features of the gravity field over the ocean (*cf.* Figs 1a and 4a). In addition, all oceanic fracture zones and transform faults are highlighted by linear and narrow gravity lows bounded by positive gravity anomalies on both sides (Fig. 4a).

At the basin scale (Fig. 4b), the most pronounced feature is the negative gravity anomaly in the SE over the continent (less than -70 mGal), which is bounded by a series of coast-parallel positive anomalies offshore. In the Møre and Vøring Basins, the positive gravity anomalies and structural highs of the crystalline basement correlate spatially (*cf.* Figs 1b and 4b). In the oceanic domain, the gravity field shows two positive anomalies west of the marginal highs. Reduced gravity over the Jan Mayen Fracture Zone separates the oceanic positive anomalies and is especially distinct as a steep NW–SE oriented gradient at the NW side of the oceanic anomaly. Towards the continent, in the area of the Jan Mayen Lineament, this NW–SE trending gravity low widens over the Møre Basin.

2.3 Densities

Densities used for gravity modelling are set constant within each layer (Table 1, Fig. 5) and are based on density logs of industrial boreholes (NPD 2007) and on literature values (Berndt *et al.* 2001; Mjelde *et al.* 2001, 2005; Torne *et al.* 2003; Fernandez *et al.* 2005; Tsikalas *et al.* 2005; Ebbing *et al.* 2006; Raum *et al.* 2006). Furthermore, the derived densities are in the range of the empirical velocity–density relationship from Barton (1986) for

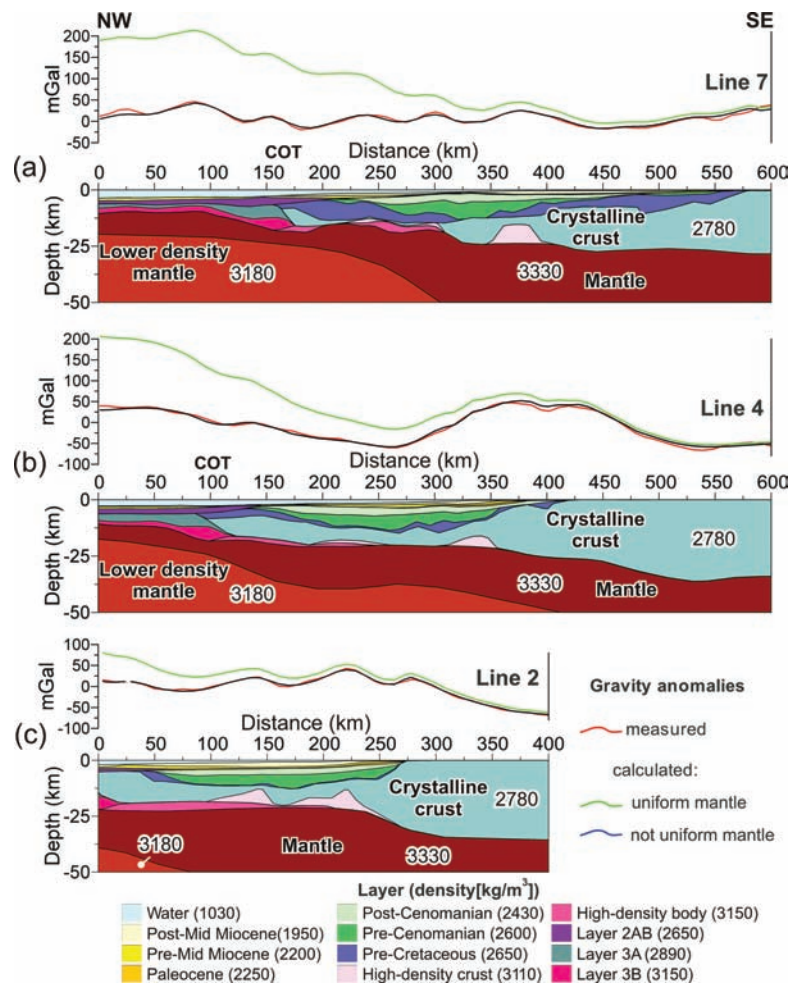


Figure 5. Representative slices through the 3-D gravity model highlighting the misfit between calculated and observed gravity anomalies assuming a homogeneous mantle below the continental and oceanic crust and one end-member geometry of a density contrast between the continental and oceanic upper mantle (for location see Figs 1(b), 3(b), 8 and 9(c)). (a) Line 7 across Vøring Basin, (b) Line 4 along Jan Mayen Lineament and (c) Line 2 across Møre Basin. COT: continent ocean transition.

crustal–mantle rocks. The Cenozoic sediments are characterized by low densities as they have a low degree of compaction. Higher densities were assigned to the Cretaceous layers according to their greater burial depth and compaction and the highest sediment density corresponds to the strongly compacted pre-Cretaceous. The continental crystalline crust was assigned a density of 2780 kg m^{-3} according to the observed P -wave velocities and published 2-D gravity models. In contrast, a relative high density of 3150 kg m^{-3} is assigned to the lower crustal high-velocity body beneath the Vøring Basin consistent with previous studies (Mjelde *et al.* 2005; Raum *et al.* 2006). Based on the resemblance of seismic velocities between the continental high-velocity body and the oceanic layer 3B, the same density was given to both. Likewise, density values for the other two oceanic layers (2AB and 3A) were assigned in accord with earlier studies (Mjelde *et al.* 2005; Raum *et al.* 2006).

3 3-D GRAVITY MODELLING AND STRIPPING

3.1 Method

3-D gravity modelling and stripping were performed with the Interactive Gravity and Magnetic Application System (IGMAS), which

allows the calculation of the total gravity response from a 3-D structural model by triangulation between predefined structural levels along parallel 2-D vertical slices (Götze 1978; Götze & Lahmeyer 1988; Schmidt & Götze 1998). The geometrical approximation for each 3-D structural layer is determined by multiple polyhedra with triangulated facets between the top and the base of each layer. Therefore, the calculated gravity effect of the 3-D structural model is the sum of gravity effects of all triangulated polyhedra.

In practise, the 3-D gravity modelling was carried out by interactive changes in the geometry and density of the layers below Base Cretaceous along 16 NW–SE-oriented working planes through the 3-D structural model. Three key examples of these working planes are illustrated in Fig. 5. The position of the working planes has been chosen perpendicular to the main structural features of the Norwegian continental margin, crossing the most important gravity lows and highs (Fig. 4a). This configuration of the working planes was chosen to minimize possible artefacts due to 3-D triangulation between vertical planes. In order to avoid any problems related to the geometry of the model, which cuts at an angle to the margin and across the major crustal boundaries, the lateral extension of the model is 6000 km in all directions exceeding the study area. In addition, the regional features of the North Atlantic region have been schematically included into the laterally extended parts of the

3-D structural model. Downward, our 3-D model includes the lithospheric mantle for which several configuration of the lithosphere–asthenosphere boundary have been evaluated (Scheck-Wenderoth & Maystrenko 2008). As for all models studied more than 60 per cent of the model volume consists of mantle material, a reference density of 3200 kg m^{-3} has been chosen as an average model density. Anomalous densities of the model layers, calculated with regard to this reference density, vary by more than -700 kg m^{-3} for the sediments and less than -400 kg m^{-3} for the crystalline crust.

To evaluate the deep structure of the margin we apply gravity stripping. The main purpose of the 3-D gravity stripping was to remove the gravity effect of the shallow and well-constrained layers from the observed gravity field above selected levels of the 3-D model and to assess the gravity effect of the underlying layers. This is especially important for the Norwegian continental margin where the gravity signal of the upper mantle structure is masked by the thick sediments of the margin and the thick crust beneath the continent. To calculate the residual gravity field to the base of crust, the following work sequence was applied during 3-D gravity stripping. First, the density values of all layers below the base of the “stripped” layers were set to the reference density of the 3-D model (3200 kg m^{-3}). Subsequently, the gravity effect of the layers that had to be “stripped” was calculated. Finally, this modelled gravity effect of the selected layers was subtracted from the observed gravity to obtain the residual gravity signal originating from the deeper layers.

3.2 Results

As a first step, the gravity response of the unchanged 3-D structural model of Scheck-Wenderoth *et al.* (2007) has been examined. Besides the configuration of the sedimentary fill and of the crystalline crust, a high-density body beneath the Vøring Basin has been included corresponding geometrically to the high-velocity body observed in deep seismic data. The gravity response of this initial 3-D structural model assuming a homogenous mantle density of 3300 kg m^{-3} is in good agreement with the large-wavelength field observed over the Vøring Basin, but fails to reproduce the observed gravity anomaly over the western Møre Basin and some of the short-wavelength anomalies across the margin. Moreover, a large misfit between model and observation was obtained for the oceanic domain.

3.2.1 Continental domain

To obtain a good fit between modelled and observed gravity, two major modifications were needed in the continental part.

First, an additional high-density body had to be included in the lower crust of the western Møre Basin (Fig. 6b). The 3-D geometry of this body was determined by gravity modelling since deep seismic control is limited (Fig. 2). Its shape is similar to the one considered below the western Vøring Basin and approximately consistent with a previous gravity study covering the continental part of the margin (Ebbing *et al.* 2006). In addition, the modelled high-density body beneath the Møre Basin is consistent with the limited deep seismic data available across the western Møre Basin (Raum *et al.* 2006; Mjelde *et al.* 2009) that indicate the presence of a high-velocity body, similar to the one below the Vøring Basin. No high-density body is required along the Jan Mayen Lineament to fit the observed gravity signal. The two lower crustal high-density bodies show the same left lateral offset along the Jan Mayen Lineament as observed in the other crustal layers. Comparably to the results from the deep seismic data we find that the lower crustal high-density bodies appear to be geometrically continuous with the lowermost oceanic crustal layer 3B. Accordingly, the thickness of the lower crustal high-density bodies (Fig. 6b) matches well with the thickness of the oceanic layer 3B (Fig. 6a) and the two maps appear cut apart along the continent–ocean boundary. Based on similarities in seismic velocities and spatial position, the same density has been assigned to these high-density bodies and to the oceanic layer 3B (Fig. 6a). Consequently, the modelled oceanic layer 3B and the lower crustal high-density bodies represent one lower crustal layer of high-density extending laterally from the lower crust beneath the western Vøring and Møre Basins to the oceanic part of the model.

Secondly, isolated high-density zones (3110 kg m^{-3}) had to be incorporated in the lower continental crust to reproduce the short-wavelength undulations of the observed gravity field in the eastern part of the Vøring and Møre Basins. The thickness distribution of the latter (Fig. 6c) shows that these bodies form narrow, NNE–SSW trending structures below some prominent structural highs of the crystalline basement. The thickest of these high-density zones ($>10 \text{ km}$) is modelled beneath the Utgard High which is associated with the highest values of the gravity field (80 mGal) observed in the Vøring Basin (Fig. 4). There, crystalline basement rocks reach

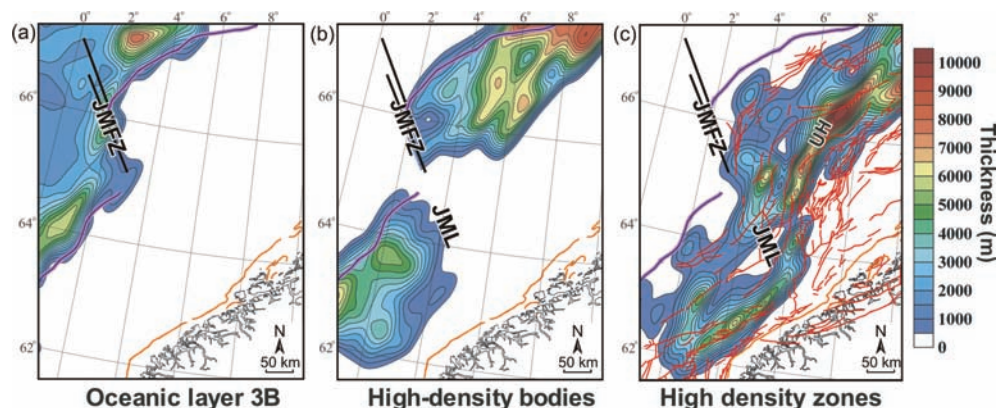


Figure 6. Thicknesses of the oceanic layer 3B (a) and continental lower crustal high-density bodies (b). (c) Thickness map of the high-density zones within the continental crust with location of the major basement faults (red lines; after Blystad *et al.* 1995). For legend see Fig. 3. JMFZ: Jan Mayen Fracture Zone, JML: Jan Mayen Lineament, UH: Utgard High.

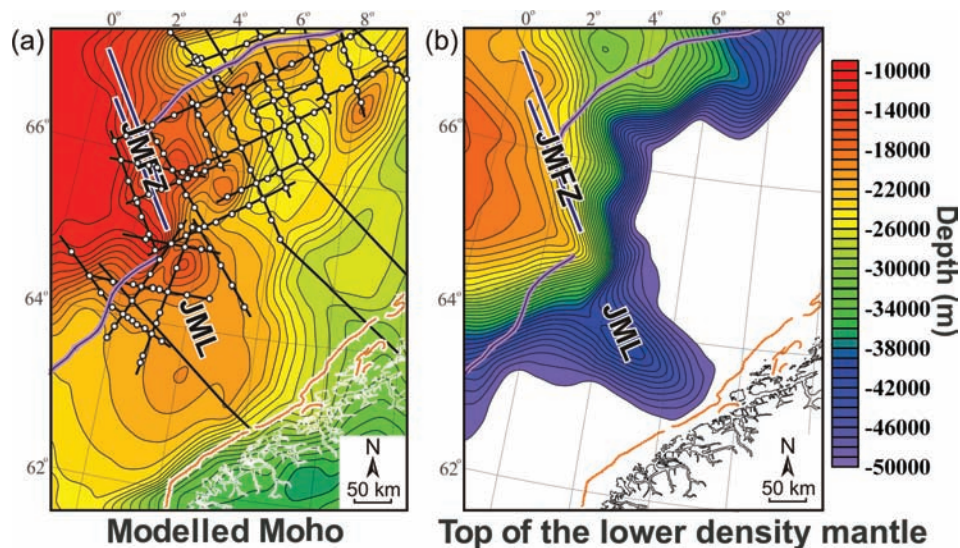


Figure 7. (a) Modelled depth to Moho based on data from Ottemoller & Midzi (2003) and Raum *et al.* (2006). Black lines are the wide-angle seismic profiles and white circles correspond to position of OBSs. (b) Top of the lower density mantle in the modelled end-member geometry of the density contrast between continental and oceanic upper mantle. For legend see Fig. 3. JMFZ: Jan Mayen Fracture Zone, JML: Jan Mayen Lineament.

a very shallow level and are intruded by sills with P -wave velocities of more than 7000 m s^{-1} (Berndt *et al.* 2000).

Gravity modelling in itself is characterized by an inherent ambiguity. The uncertainty that a variety of density models can fit the observed data of a given gravity field can be reduced if independent constraints from OBS data are taken into account. As mentioned earlier, such data (e.g. Mjelde *et al.* 2002; Raum *et al.* 2006) safely constrain the high-density body in the lower crust beneath the Vøring Basin. On the other hand, the shape of the high-density body beneath the SW part of the Møre Basin derived by gravity modelling is constrained by wide-angle seismic lines only beneath the northern part of the Møre Basin (Mjelde *et al.* 2009). Therefore, some uncertainties remain within the SW Møre Basin. Unfortunately, the absence of densely spaced constraints for the Moho beneath the SW Møre Basin adds to this ambiguity (see Fig. 2) in this part of the study area (Fig. 7a).

In general, the Moho is deeper than 38 km beneath the continent, less than 10 km deep beneath the oceanic crust and displays pronounced short-wavelength undulations beneath the Vøring Basin (Fig. 7a). Accordingly, the continental crust between top basement and Moho is thinned to a few km towards the continent–ocean transition.

3.2.2 Oceanic domain

After having obtained a reasonably good fit between modelled and observed gravity in the continental part, a large misfit was left over the oceanic domain. A uniform density in the upper mantle below the continental and the oceanic domains imposes a long-wavelength positive anomaly over the oceanic domain that is up to 180 mGal larger than observed (Fig. 5). This misfit calls for a less dense mantle below the oceanic domain than below the continental crust. As the geometry of the transition between these two areas of different upper mantle density is unknown and gravity inversion is non-unique, we examined several possible end-member geometries for the transition between denser continental and less dense oceanic upper mantle, using the same crustal configuration. In summary, all

models were robust concerning the required lateral density contrast in the lithospheric mantle.

One possible configuration (Fig. 5) was chosen to mimic a thermal zonation. In this model a wedge of high-density upper mantle with a density of 3330 kg m^{-3} thins out in the upper part below the oceanic crust. The less dense mantle was placed into the lower oceanic part of the model and has a density of 3180 kg m^{-3} (Fig. 7b). Fig. 8(a) shows the calculated gravity obtained from this model and demonstrates that all major features of the observed gravity are reproduced. Fig. 8(b) displays the gravity difference after subtracting the modelled gravity from the observed gravity (Fig. 4b) and illustrates the degree of consistence between model and observation. The difference between observed and modelled gravity is in the range of $\pm 10 \text{ mGal}$ for the largest part of the residual gravity map (Fig. 8b). The few larger misfits are due to the spacing of the vertical slices and occur localized between the slices. These misfits do not have a strong impact on the regional gravity field of the study area but are shown to allow a quantitative assessment of the method's limitations. The gravity response for the model in map (*cf.* Figs 4b and 8a) and cross-sectional views (Fig. 5) demonstrates that a good fit is obtained with the observed gravity data in terms of regional structure.

3.2.3 Gravity stripping

The next step of the gravity modelling consisted of 3-D gravity stripping. The crust-free gravity anomalies (Fig. 9a) represent the residual gravity field with the effect of sea water, sediments and crystalline crust removed. Though a long wavelength trend is discernible with negative anomalies over the ocean and positive anomalies over the margin and continent, an additional complex pattern of short-wavelength gravity anomalies is present in this map. A comparison of these short-wavelength features with the pattern found in the residual gravity map (Fig. 8b) indicates that they may be related to smaller crustal heterogeneities that are not properly resolved by the model.

The gravity low in the SE part of the map (Fig. 9a) is produced by the deep Moho position beneath the continent. Although the

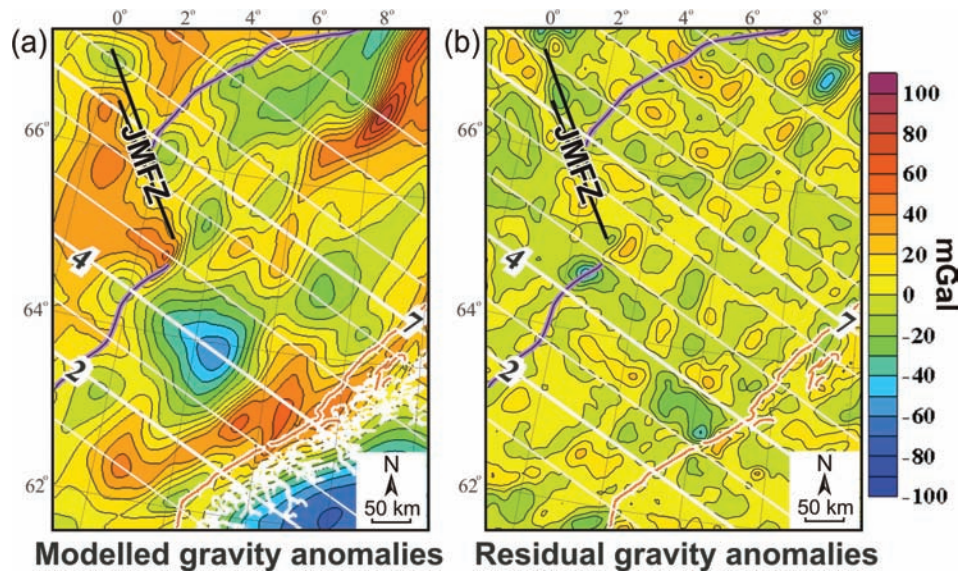


Figure 8. (a) Modelled gravity anomaly maps with the location of vertical slices through the 3-D structural model. (b) Residual gravity map representing difference between the modelled Fig. 8(a) and the observed gravity field (Fig. 3b). For legend see Fig. 3. JMFZ: Jan Mayen Fracture Zone, JML: Jan Mayen Lineament.

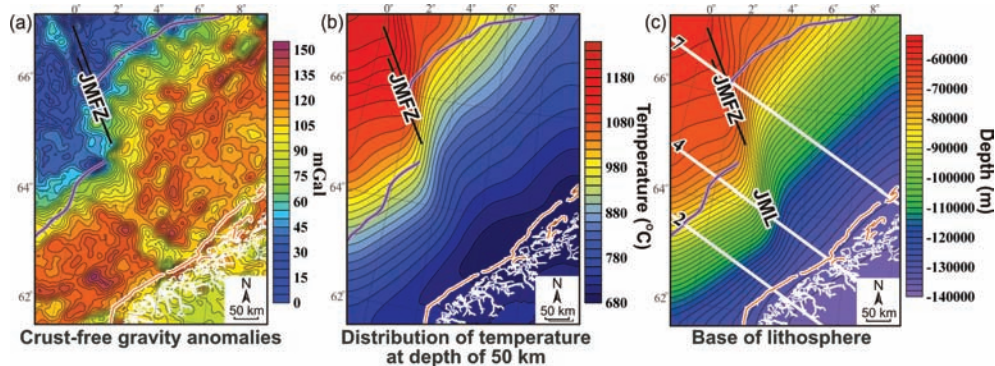


Figure 9. (a) Crust-free anomalies—residual gravity field obtained after subtraction of the gravity effects due to sea water, sediments and the crystalline crust from the observed gravity field. (b) Temperature (in °C) at 50 km depth predicted by 3-D temperature modelling (Scheck-Wenderoth & Maystrenko 2008). (c) Base of the lithosphere considered for 3-D thermal modelling (Scheck-Wenderoth & Maystrenko 2008) characterized by a continuous slope from the continent to the ocean beneath the continental margin and obtained by interpolation between the calculated oceanic lithosphere (after Zhang & Lay 1999) and continental lithosphere (after Artemieva *et al.* 2006). For legend see Fig. 3. JMFZ: Jan Mayen Fracture Zone, JML: Jan Mayen Lineament.

influence of the crustal structure has been subtracted, the ‘missing’ mantle material is producing a low relative to the margin, where the upper mantle is shallower than beneath the Caledonides. In contrast, no such explanation holds for the gravity low obtained for the oceanic part as the Moho there is far shallower and the systematic long-wavelength difference of the subcrustal gravity signal requires different upper mantle densities beneath the two domains.

Scheck-Wenderoth & Maystrenko (2008) calculated the 3-D conductive thermal field of the Norwegian continental margin using the same configuration of the model for the crustal part and obtained considerably higher temperatures in the lithospheric mantle beneath the oceanic than beneath the continental crust (Fig. 9b). The respective 3-D thermal model assumes an upper boundary condition of 2 °C at the present-day surface/seafloor and a lower boundary condition of 1300 °C at the lithosphere–asthenosphere boundary. These results indicate that a rather thin lithosphere (60–70 km, Fig. 10c) has to be present in the oceanic part to reproduce observed temperature and heat flow data and to be consistent with seismological data from surface wave inversion. In response to this

shallow lithosphere–asthenosphere boundary beneath the ocean, the lithospheric mantle is considerably hotter than beneath the continent. Comparing the maps of the crust-free-anomalies (Fig. 9a) and the temperature distribution at 50 km depth (Fig. 9b), the spatial correlation of low gravity and high temperatures in the oceanic domain is obvious. This correlation indicates that density reduction in the mantle beneath the ocean may be related to an increase in temperature with depth.

4 COMBINED 3-D THERMAL/GRAVITY MODELLING

To test the hypothesis of a thermally induced density reduction in the lithospheric mantle, combined 3-D thermal and gravity modelling has been carried out. A procedure was applied previously proposed by Breivik *et al.* (1999) for two seismic profiles in the western Barents Sea. Breivik *et al.* (1999) showed that the reduction of mantle densities across the continent–ocean transition can

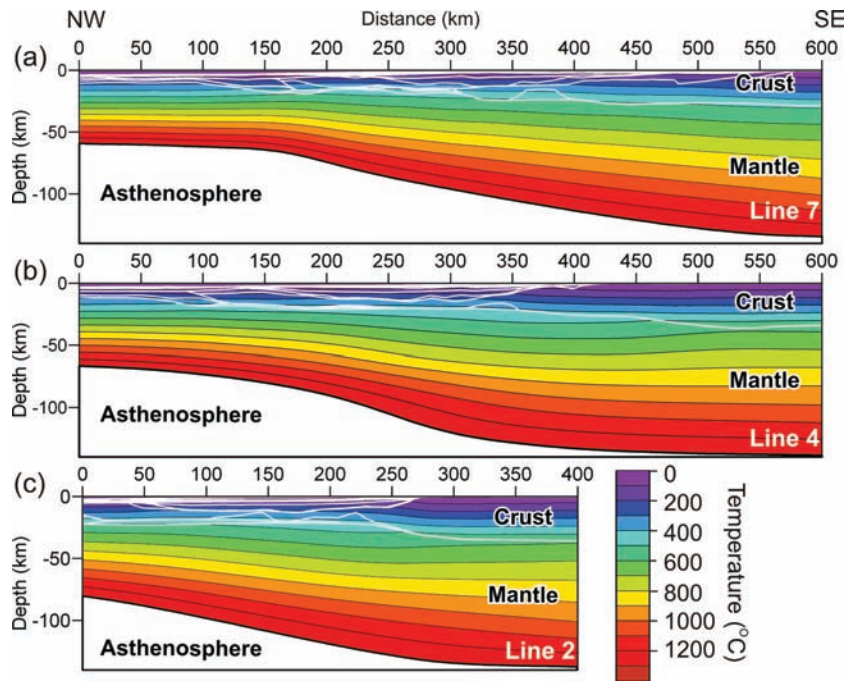


Figure 10. Vertical slices through the 3-D thermal model (Scheck-Wenderoth & Maystrenko 2008) along the same profiles as in Fig. 5. White lines outline the configuration of the crust. For location see Figs 1(b), 3(b), 8 and 9(c).

be explained as being a function of thermal expansivity affecting the mantle rocks at high temperatures. To quantify the influence of thermal expansivity for our model, three temperature profiles (Fig. 10) have been extracted from the 3-D thermal model (Scheck-Wenderoth & Maystrenko 2008). The location of these profiles has been chosen to be identical with the position of three representative slices through the 3-D gravity model in Fig. 5 (Lines 2, 4 and 7). In these profiles, the initial layer representing the lithospheric mantle in the model has been subdivided into eight layers defined geometrically by 100 °C intervals of temperature. For these individual mantle layers the density reduction in response to the thermal expansivity was calculated according to $\rho(T) = 3300(1 - \alpha T)$, where 3300 [kg m⁻³] is the density of mantle rocks at 0 °C, $\alpha = 3.2 \times 10^{-5}$ [°C⁻¹] is the volume coefficient of thermal expansion and T [°C] is temperature. Subsequently, the geometry of these individual mantle layers for the 3-D model portion between Lines 2 and 7 was obtained by lateral interpolation between the profiles.

Fig. 11 shows the gravity response of the resulting model considering the effect of thermal expansivity. The large-scale pattern of modelled and measured gravity shows a good correlation and supports the hypothesis of a thermally induced density reduction in the oceanic lithospheric mantle with respect to the continent. There is, however, some misfit left between the thermally motivated gravity model and observation that reaches up to 50 mGal. This could be related to uncertainties concerning the depth to the base of the lithosphere beneath the continental margin and one possibility to improve this fit is to reconsider the geometry of the lithosphere–asthenosphere boundary. The depth to the lithosphere–asthenosphere boundary beneath the oceanic part has been derived according to lithospheric age—Love and Rayleigh wave phase velocity relations (Zhang & Lay 1999), and the lithosphere thickness beneath the continent is inferred from global heat flow studies and seismologic data (Artemieva *et al.* 2006). In contrast, beneath the continental margin itself, there are no direct data concerning the depth to the lithosphere–asthenosphere boundary.

Scheck-Wenderoth & Maystrenko (2008) have applied interpolation between the oceanic and onshore parts to fill this gap. Therefore, a modification of the depth to the lithosphere–asthenosphere boundary beneath the Vøring and Møre Basins may be justified to improve the fit between measured and modelled gravity. Introducing a steeper gradient in lithospheric thickness between the continental and oceanic domains results in a very good match between model and observation (sufficient to fit the measured gravity; Fig. 12). In the respective model, the base of the lithosphere has been changed below the continental margin to account for a steeper gradient of depth change close to continent–ocean transition, while the lithosphere thickness beneath the continent and the ocean has been preserved in the previous (data-supported) state (Fig. 11).

5 DISCUSSION

The evaluation of the deep density structure at the Norwegian passive margin using 3-D gravity modelling revealed two types of first order density heterogeneities: (1) density heterogeneities present in the lower crust and (2) a density contrast within the upper lithospheric mantle between the continental and the oceanic parts of the system.

5.1 Density heterogeneities in the lower crust

We find two different types of structures with anomalous high density in the lower crust of the Norwegian margin, namely two isolated high-density bodies (HDB) beneath the western Vøring and Møre Basins, adjacent to the continent–ocean transition (Fig. 6b) and several NNE–SSW trending high density zones (HDZ) beneath the eastern Vøring and Møre Basins (Fig. 6c).

The HDB coincide spatially with high-velocity bodies observed in seismic data (Mjelde *et al.* 2005; Raum *et al.* 2006) and have partially been reported in former gravity studies of the continental part of the margin (Torne *et al.* 2003; Fernandez *et al.* 2005; Ebbing

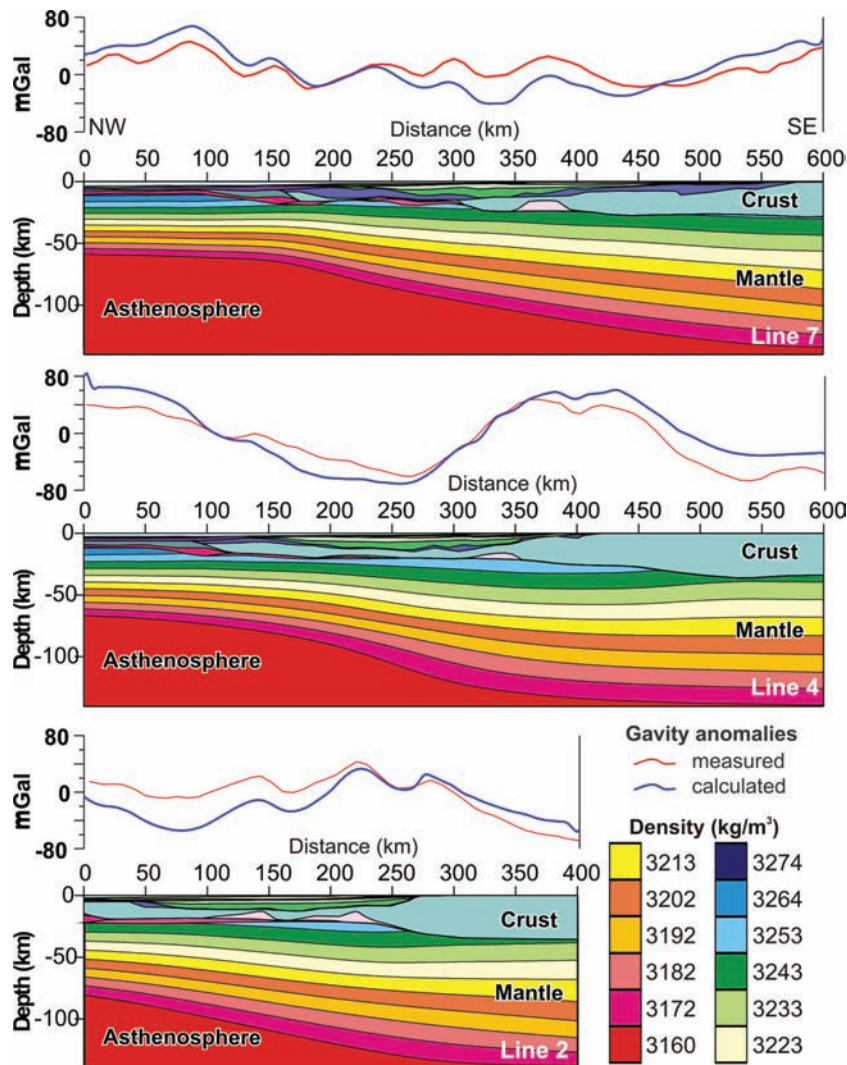


Figure 11. Results of combined 3-D thermal/gravity modelling along the profiles shown in Fig. 10 with thermally differentiated mantle densities for the interpolated base of the lithosphere (Fig. 9c) between the oceanic and continental domains. For location see Figs 1(b), 3(b), 8 and 9(c).

et al. 2006). Moreover, similar high-density–high-velocity bodies have been observed at other passive volcanic margins underneath seaward-dipping reflector sequences close to the continent–ocean transition (Bauer *et al.* 2000; Franke *et al.* 2007; Hirsch *et al.* 2007). Accordingly, a common interpretation for the HDB (Fig. 6b), is that they represent the relicts of breakup-related underplating of mantle melts intruded into the lower crust. For the Norwegian margin, such an interpretation is further supported by the continuity of the HDB within oceanic layer 3B (Fig. 6a), in terms of geometry and physical properties. Breakup-related volcanics drilled in the area above these bodies imply a pre- or syn-breakup age (Palaeocene) for their formation (Skogseid *et al.* 2000). Another observation backing the underplating concept is that a breakup-related origin of high-density lower continental crust has also been inferred beneath the conjugate margin in southeast Greenland (Korenaga *et al.* 2001) and volcanic products found at both continental ends of the Jan Mayen Fracture Zone are similar in age and composition (Torsvik & Prestvik 1991).

An alternative interpretation of the high-density bodies is that they represent eclogites, which formed in the lower crust during the Caledonian orogeny and were dismembered during later extensional

phases (Gernigon *et al.* 2006). Yet, some observations strengthen the case against eclogites as cause for the positive gravity anomalies. First, in particular at the continent–ocean transition, the presence of eclogites is difficult to reconcile with the continuity between the HDB with oceanic layer 3B. Second, the volcanics drilled on the Norwegian margin do not contain any evidence for REEs (rare-earth elements) typical for garnet-containing eclogites, which should be present if breakup took place through an eclogitic lower crust (J. Hertogen 2007, personal communication).

Nevertheless, the concept of dismembered eclogites may hold as interpretation for the linear NNE–SSW oriented HDZ (Fig. 6c) found beneath the eastern half of the Vøring and Møre Basins. Multichannel seismic data indicate large listric detachment faults dipping westward beneath the Vøring Basin (Osmundsen *et al.* 2002) that have accommodated the Mesozoic extension of the margin. The traces of these major faults affecting the base Cretaceous (Fig. 6c) coincides spatially with the steep gradients in thickness distribution of the HDZ. In addition, these zones not only coincide with basement highs but moreover, they follow the Caledonian structural trend and are located in areas where no breakup-related volcanics are observed. If the HDZ were related to the activity of the

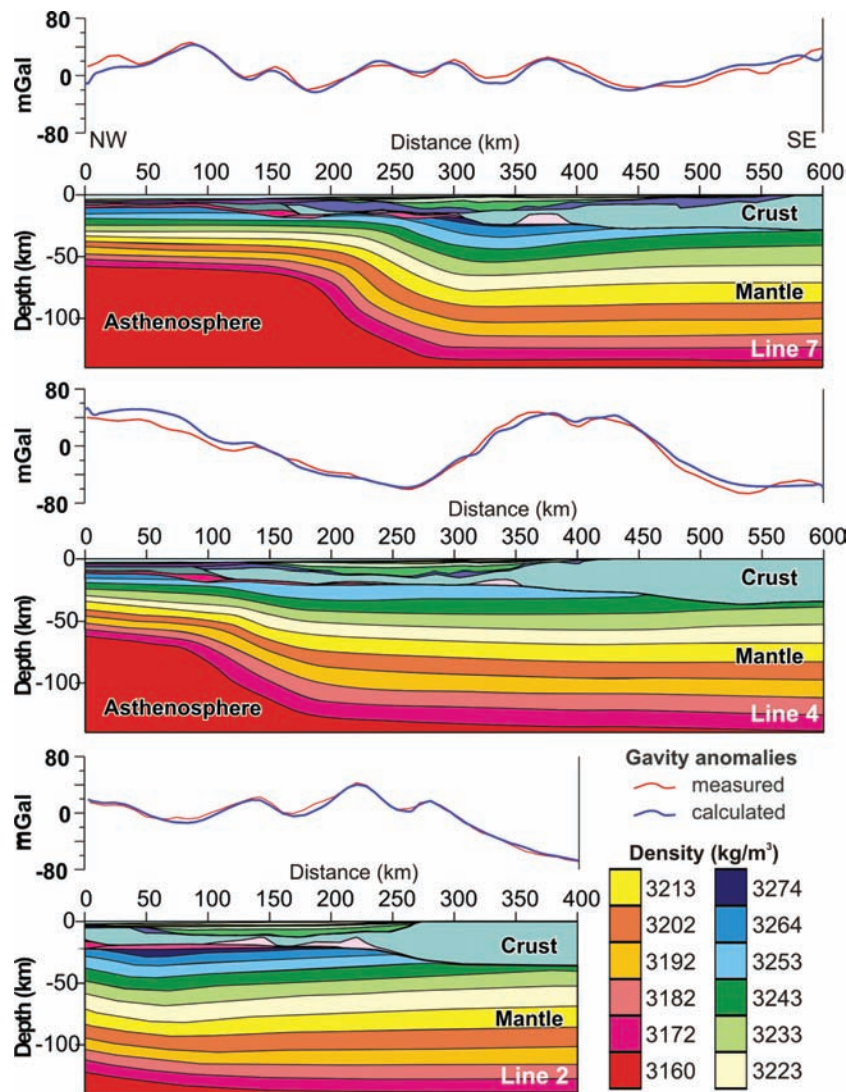


Figure 12. Results of combined 3-D thermal/gravity modelling along profiles located as in Fig. 10 but with modified geometry of the lithosphere–asthenosphere boundary beneath the margin. The configuration of the base lithosphere is adjusted to improve the fit with observed gravity, assuming homogeneous composition but temperature-dependent densities of the mantle. For location see Figs 1(b), 3(b), 8 and 9(c). Note the steep gradient in depth of the 1300 °C isotherm across the continent–ocean transition in lines 4 and 7.

NNE–SSW trending faults, this would imply a pre-breakup age of their generation.

5.2 Density heterogeneities in the upper lithospheric mantle

The most significant result of our study is that the oceanic mantle appears to be less dense than the continental one. This is in line with previous 2-D gravity models of the North Atlantic Ocean (Breivik *et al.* 1999; Ritzmann *et al.* 2002; Schmidt-Aursch & Jokat 2005). The simplest explanation for this density difference is a thermal effect. Thermally induced density reduction in the oceanic mantle near the Norwegian margin could be a result of increasing mantle temperatures towards the Mid-Atlantic Ridge and towards the Iceland plume (Maclennan *et al.* 2005; Parkin *et al.* 2007). Alternatively, convection processes in the asthenospheric mantle could prevent thickening of the oceanic mantle lithosphere to a thickness predicted by the half-space cooling model. 3-D thermal modelling (Scheck-Wenderoth & Maystrenko 2008) and surface wave

inversion along ray paths extending from the margin out to the Mid-Atlantic Ridge (Midzi *et al.* 1999) suggest that the thickness of the oceanic lithosphere (60–70 km) is reduced with respect to the prediction of the half-space cooling model (90 km). If this shallow lithosphere–asthenosphere boundary coincides with the 1300 °C isotherm, a considerably higher heat flow and elevated temperatures in the oceanic lithosphere, compared to the continent, would be the consequence. Accordingly a hotter and less dense upper mantle would be present beneath the ocean, than beneath the continent.

On the other hand, models of the thermal evolution of the Vøring margin (Gernigon *et al.* 2006) indicate that breakup-induced heating did not last very long after the Eocene due to the westward migration of lithospheric extension. Thus, a thermal effect may not be sufficient to account for the present-day gravity signal and the latter could be additionally related to compositional differences. This option has not been further explored in this study. Nevertheless, we find minor inconsistencies between the thermal and the gravity models for the area around the continent–ocean transition

(Fig. 11). While the thermal model (Fig. 10) suggests a moderate slope of the lithosphere–asthenosphere boundary between the continent and the ocean, the gravity model considering density reduction due to thermal expansivity requires a steeper gradient between oceanic and continental lithosphere thickness (Fig. 12). This mismatch may be either due to a sharp change in lithosphere thickness across the continent–ocean transition or it may be related to compositional variations not considered in the modelling. If the sharp transition from continental to oceanic lithosphere was real, it would imply a considerable thermal gradient below the base of the lithosphere at the continent–ocean transition and an interesting question would be which mechanism could be responsible for that? One possible explanation predicted by numerical models (e.g. van Wijk *et al.* 2004; Huisman & Beaumont 2008) is the relatively steep boundary between continental lithosphere and ascending sublithospheric material during breakup. In this case, rapid thinning of the lithosphere beneath the continent–ocean transition (Fig. 12) reflects the result of post-breakup cooling within the area which was adjacent to the breakup axis in Palaeocene.

5.3 Density heterogeneities along the Jan Mayen Fracture Zone/Jan Mayen Lineament

The gravity models also indicate reduced mantle densities in the lower crust beneath the Jan Mayen Lineament (Figs 5 and 7b) that is located along the continent-ward prolongation of the oceanic Jan Mayen Fracture Zone. At the larger scale, the Jan Mayen Fracture Zone is characterized by a linear negative gravity anomaly observed over the northern Atlantic Ocean (Fig. 4a). According to plate reconstructions (Torsvik *et al.* 2002), last movements along the Jan Mayen Fracture Zone are related to the final separation of the Jan Mayen microcontinent from East Greenland in the Miocene. This was long after continental breakup at the Norwegian continental margin and indicates that this oceanic fracture zone is tectonically younger than neighbouring domains at the Norwegian continental margin. In contrast, the continental Jan Mayen Lineament may be of pre-breakup age according to the concept of Torske & Prestvik (1991). They proposed that the continental Jan Mayen Lineament may have acted as a lithosphere-penetrating strike-slip transfer fault or accommodation zone during Mesozoic phases of extension and thus would be older than breakup. This implies that the continental Jan Mayen Lineament may have been the precursor of the Jan Mayen Fracture Zone and could play as a deep lithospheric conduit which is responsible for transport of volatiles from the asthenosphere to the upper mantle (Torske & Prestvik 1991). Thus the reduced densities along the Jan Mayen Lineament could result from the superimposed effects of pre-breakup tectonic activity and possible later heating related to the development of the Jan Mayen Fracture Zone. Finally, a deep crustal root beneath the lineament would produce the same gravity signal as a zone of reduced upper mantle density. Although our models clearly demonstrate the need for a deep crustal and/or upper mantle mass deficit along the Jan Mayen Lineament we cannot discriminate between an upper mantle of (thermally) reduced densities and the presence of a continuous crustal root along this lineament, as this would require additional deep seismic constraints.

6 CONCLUSIONS

3-D gravity modelling indicates two types of density heterogeneities in the deeper parts of the Norwegian passive continental margin: a

less dense oceanic lithospheric mantle compared to the continent, two isolated high-density bodies beneath the western Vøring and Møre Basins and several NNE–SSW trending high-density zones beneath the eastern Vøring and Møre Basins.

Furthermore, 3-D lithospheric-scale models consistent with both the thermal and the gravity fields indicate that the transition between continental and oceanic lithosphere is sharp with a steep gradient in thickness beneath the continent–ocean transition.

A local mass deficit in the lower crust–upper mantle along the Jan Mayen Lineament could be related to increased temperatures and/or compositional changes beneath the lineament compared to the adjacent parts of the continental domain.

ACKNOWLEDGMENTS

This work was supported by the German Science Foundation DFG, and by the European Science Foundation (ESF) under the EURO-CORES Programme EUROMARGINS, with support from the European Commission (6th Framework Programme, contract ERAS-CT-2003–980409). We thank T. Raum, R. Mjelde, J. I. Faleide, H. Brekke, H. Thybo, and J. Ebbing for supplying data and for fruitful discussions as well as H.-J. Götze and S. Schmidt for the 3-D gravity modelling software (IGMAS). We thank Keith Louden, Tim Minshull and two anonymous reviewers for constructive reviews and comments, which helped to improve the original version of the manuscript.

REFERENCES

- Artemieva, I.M., Thybo, H. & Kaban, M.K., 2006. Deep Europe today: geophysical synthesis of the upper mantle structure and lithospheric processes over 3.5 b.y., in *European Lithosphere Dynamics*, Geological Society of London Memoir 32, pp. 14–41, eds Gee, D. and Stephenson, R., The Geological Society Publishing House, Bath.
- Barton, P.J., 1986. The relationship between seismic velocity and density in the continental crust—a useful constraint? *Geophys. J. R. astr. Soc.*, **87**, 195–208.
- Bauer, K. *et al.*, 2000. Deep structure of the Namibia continental margin as derived from integrated geophysical studies, *J. Geophys. Res., B, Solid Earth Planets*, **105**(11), 25 829–25 853.
- Berndt, C., Skogly, O.P., Planke, S., Eldholm, O. & Mjelde, R., 2000. High-velocity breakup-related sills in the Voring Basin, off Norway, *J. Geophys. Res., B, Solid Earth Planets*, **105**, 28 443–28 454.
- Berndt, C., Mjelde, R., Planke, S., Shimamura, H. & Faleide, J.I., 2001. Controls on the tectono-magmatic evolution of a volcanic transform margin: the Voring transform margin, NE Atlantic, *Mar. Geophys. Res.*, **22**(3), 133–152.
- Blystad, P., Brekke, H., Faereth, R.B., Larsen, B.T., Skogseid, J. & Tørdubakken, B., 1995. *Structural Elements of Norwegian Continental Shelf. Part II: The Norwegian Sea Region*, The Norwegian Petroleum Directorate, Stavanger, pp. 1–45.
- Breivik, A.J., Verhoe, J. & Faleide, J.I., 1999. Effect of thermal contrasts on gravity modeling at passive margins: results from the western Barents Sea, *J. Geophys. Res., B, Solid Earth*, **104**, 15 293–15 311.
- Brekke, H., 2000. The tectonic evolution of the Norwegian Sea Continental Margin with emphasis on the Voring and More Basins, *Geol. Soc. London, Spec. Publ.*, **167**, 327–378.
- Ebbing, J., Lundin, E., Olesen, O. & Hansen, E.K., 2006. The mid-Norwegian margin: a discussion of crustal lineaments, mafic intrusions, and remnants of the Caledonian root by 3-D density modelling and structural interpretation, *J. Geol. Soc., Lond.*, **163**, 47–59.
- Fernandez, M., Ayala, C., Torne, M., Verges, J., Gomez, M. & Karpuz, R., 2005. Lithospheric structure of the mid-Norwegian margin; comparison

- between the More and Voring margins, *J. Geol. Soc., Lond.*, **162**, 1005–1012.
- Franke, D., Neben, S., Ladage, S., Schreckenberger, B. & Hinz, K., 2007. Margin segmentation and volcano-tectonic architecture along the volcanic margin off Argentina/Uruguay, *S Atlantic: Mar. Geol.*, **244**, 46–67.
- Gernigon, L., Lucazeau, F., Brigaud, F., Ringenbach, J.-C., Planke, S. & Le Gall, B., 2006. A moderate melting model for the Voring margin (Norway) based on structural observations and a thermo-kinematical modelling: implication for the meaning of the lower crustal bodies, *Tectonophysics*, **412**, 255–278.
- Götze, H.-J., 1978. Ein numerisches Verfahren zur Berechnung der gravimetrischen Feldgrößen drei-dimensionaler Modellkörper, *Arch. Met. Geoph. Biokl., Ser. A*, **25**, 195–215.
- Götze, H.J. & Lahmeyer, B., 1988. Application of three-dimensional interactive modeling in gravity and magnetics, *Geophysics*, **53**, 1096–1108.
- Hirsch, K.K., Scheck-Wenderoth, M., Paton, D.A. & Bauer, K., 2007. Crustal structure beneath the Orange Basin, *South Africa: South Africa. J. Geol.*, **110**, 249–260.
- Huisman, R.S. & Beaumont, C., 2008. Complex rifted continental margins explained by dynamical models of depth-dependent lithospheric extension, *Geology*, **36**(2), 163–166.
- IOC, IHO & BODC, 2003. *Centenary Edition of the GEBCO Digital Atlas, published on CD-ROM on behalf of the Intergovernmental Oceanographic Commission and the International Hydrographic Organization as part of the General Bathymetric Chart of the Oceans*, British Oceanographic Data Centre, Liverpool.
- Korenaga, J., Holbrook, W.S., Detrick, R.S. & Kelemen, P.B., 2001. Gravity anomalies and crustal structure across the Southeast Greenland margin, *J. geophys. Res.*, **106**, 8853–8870.
- Macleanman, J., Hulme, T. & Singh, S.C., 2005. Cooling of the lower oceanic crust, *Geology (Boulder)*, **33**, 357–366.
- Midzi, V., Singh, D.D., Atakan, K. & Havskov, J., 1999. Transitional continental-oceanic structure beneath the Norwegian Sea from inversion of surface wave group velocity data, *Geophys. J. Int.*, **139**, 433–446, doi:10.1046/j.1365-246x.1999.00960.x.
- Mjelde, R., Kodaira, S. & Sellevoll, M.A., 1997. Crustal structure of the central part of the Voring Basin, mid-Norway margin, from ocean bottom seismographs, *Tectonophysics*, **277**, 235–257.
- Mjelde, R., Digranes, P., van Schaack, M., Shimamura, H., Shiobara, H., Kodaira, S. & Næss, O., 2001. Crustal structure of the outer Voring Plateau, offshore Norway, from ocean bottom seismic and gravity data, *J. Geophys. Res.*, **106**, 6769–6791.
- Mjelde, R., Kasahara, J. & Shimamura, H., Kamimura, A., Kanazawa, T., Kodaira, S., Raum, T. & Shiobara, H., 2002. Lower crustal seismic velocity-anomalies; magmatic underplating or serpentinized peridotite? Evidence from the Voring Margin, NE Atlantic, *Mar. Geophys. Res.*, **23**(2), 169–183.
- Mjelde, R., Shimamura, H., Kanazawa, T., Kodaira, S., Raum, T. & Shiobara, H., 2003. Crustal lineaments, distribution of lower crustal intrusives and structural evolution of the Voring Margin, NE Atlantic; new insight from wide-angle seismic models, *Tectonophysics*, **369**, 199–218.
- Mjelde, R., Raum, T., Myhren, B., Shimamura, H., Murai, Y., Takanami, T., Karpuz, R. & Næss, U., 2005. Continent-ocean transition on the Voring Plateau, NE Atlantic, derived from densely sampled ocean bottom seismometer data, *J. geophys. Res.*, **110**, B05101, 1–19.
- Mjelde, R., Raum, T., Kandilarov, A., Murai, Y. & Takanami, T., 2009. Crustal structure and evolution of the outer Møre Margin, NE Atlantic, *Tectonophysics*, **468**, 224–243.
- Müller, R.D., Roest, W.R., Royer, J.-Y., Gahagan, L.M. & Sclater, J.G., 1997. Digital isochrons of the world's ocean floor, *J. geophys. Res.*, **102**(B2), 3211–3214.
- Norwegian Petroleum Directorate (NPD), 2007. The NPD's Factpages, well data summary sheets, http://www.npd.no/engelsk/cwi/pbl/en/wdss_index.htm.
- Osmundsen, P.T., Sommaruga, A., Skilbrei, J.R. & Oelsen, O., 2002. Deep structure of the Mid Norway rifted margin, *Norwegian J. Geol.*, **82**, 205–224.
- Ottmoller, L. & Midzi, V., 2003. The crustal structure of Norway from inversion of teleseismic receiver functions, *J. Seismol.*, **7**, 35–48.
- Parkin, C.J., Lunnell, Z.C., White, R.S. & Christie, P.A.F., 2007. Imaging the pulsing Iceland mantle plume through the Eocene, *Geology (Boulder)*, **35**, 93–96.
- Raum, T., 2000. Crustal structure and evolution of the Faeroe, Møre and Voring margins from wide-angle seismic and gravity data, *Dr. thesis*. University of Bergen, Bergen, Norway.
- Raum, T., Mjelde, R., Digranes, P., Shimamura, H., Shiobara, K.S., Haatvedt, G., Sorenes, N. & Thorbjornsen, T., 2002. Crustal structure of the southern part of the Voring Basin, mid-Norway margin, from wide-angle seismic and gravity data, *Tectonophysics*, **355**, 99–126.
- Raum, T., Mjelde, R., Shimamura, H., Murai, Y., Bråstein, E., Karpuz, R.M., Kravik, K. & Kolstø, H.J., 2006. Crustal structure and evolution of the southern Voring Basin and Voring Transform Margin, NE Atlantic, *Tectonophysics*, **415**, 167–202.
- Ren, S., Faleide, J.I., Eldholm, O., Skogseid, J. & Gradstein, F., 2003. Late Cretaceous-Paleocene tectonic development of the NW Voring Basin, *Mar. Petrol. Geol.*, **20**, 177–206.
- Ritzmann, O., Jokat, W., Mjelde, R. & Shimamura, H., 2002. Crustal structure between the Knipovich Ridge and the Van Mijenfjorden (Svalbard), *Mar. Geophys. Res.*, **23**, 379–401.
- Sandwell, D.T. & Smith, W.H.F., 1997. Marine gravity anomaly from Geosat and ERS 1 satellite altimetry, *J. geophys. Res.*, **102**(B5), 10 039–10 054.
- Scheck-Wenderoth, M. & Maystrenko Y., 2008. How warm are passive continental margins? A 3-D lithosphere-scale study from the Norwegian margin, *Geology*, **36**(5), 419–422.
- Scheck-Wenderoth, M., Faleide, J.I., Raum, T., Mjelde, R. & Horsfield, B., 2007. The transition from the continent to the ocean—a deeper view on the Norwegian continental margin, *J. Geol. Soc.*, **164**, 855–868.
- Schmidt, S. & Götze, H.-J., 1998. Interactive visualization and modification of 3-D models using GIS functions, *Phys. Chem. Earth*, **23**, 289–296.
- Schmidt-Aursch, M.C. & Jokat, W., 2005. The crustal structure of central East Greenland – II: from the Precambrian shield to the recent mid-oceanic ridges, *Geophys. J. Int.*, **160**(2), 753–760.
- Skogseid, J., Planke, S., Faleide, J.I., Pedersen, T., Eldholm, O. & Neverdal, F., 2000. NE Atlantic continental rifting and volcanic margin formation, in *Dynamics of the Norwegian Margin*, pp. 55–82, ed. Nottvedt, A.E.A., Geol. Soc. London, Spec. Publ. 167.
- Torne, M., Fernandez, M., Wheeler, W. & Karpuz, R., 2003. Three-dimensional crustal structure of the Voring Margin (NE Atlantic): a combined seismic and gravity image, *J. geophys. Res.*, **108**, 2115–2126.
- Torske, T. & Prestvik, T., 1991. Mesozoic detachment faulting between Greenland and Norway; inferences from Jan Mayen fracture zone system and associated alkalic volcanic rocks, *Geology*, **19**(5), 481–484.
- Torsvik, T.H., Carlos, D., Mosar, J., Cocks, L.R.M. & Malme, T., 2002. Global reconstructions and North Atlantic palaeogeography 400 Ma to recent, in *BATLAS—Mid Norway Plate Reconstructions Atlas with Global and Atlantic Perspectives*, pp. 18–39, eds Eide, E.A. et al., Geological Survey of Norway.
- Tsikalas, F., Elderholm, O. & Faleide, J.I., 2005. Crustal structure of the Lofoten-Vesteralen continental margin, off Norway, *Tectonophysics*, **404**, 151–174.
- van Wijk, J.W., van der Meer, R. & Cloetingh, S.A.P.L., 2004. Crustal thickening in an extensional regime: application to the mid-Norwegian Voring margin, *Tectonophysics*, **387**(1–4), 217–228.
- Wybraniec, S., Zhou, S., Thybo, H., Forsberg, R., Perchuc, E., Lee, M., Demianov, G.D. & Strakhov, V.N., 1998. New map compiled of Europe's gravity field, *EOS, Trans., Am. geophys. Un.*, **79**(37), 437–442.
- Zhang, Y.S. & Lay, T., 1999. Evolution of oceanic upper mantle structure, *Phys. Earth planet. Inter.*, **114**, 71–80.